References and Notes

1. T. Minakami, in *Physical Volcanology*, vol. 6 of *Developments in Solid Earth Geophysics*, L. Civetta, P. Gasparini, G. Luongo, A. Rapolla, Eds. (Elsevier, Amsterdam, 1974), pp. 313–333; D. Shimozuru, in *The Surveillance and Prediction of Volcanic Activity* (Unesco, Paris, 1972), pp. 19–45.
2. S. D. Malone, E. T. Endo, C. S. Weaver, J. W. Ramey, *U.S. Geol. Surv. Prof. Pap. 1250* (1981), p. 803.
3. C. S. Weaver, W. C. Grant, S. D. Malone, E. T. Endo, *ibid.*, p. 109.
4. S. D. Malone, C. Boyko, C. S. Weaver, *Science* **221**, 1376 (1983).
5. W. W. Chadwick, Jr., D. A. Swanson, E. Y. Iwatsubo, C. C. Heliker, T. A. Leighley, *ibid.*, p. 1378.
6. D. Dzurisin, J. A. Westphal, D. J. Johnson, *ibid.*, p. 1381.
7. The velocity model at Mount St. Helens has a surface layer with a velocity of 3.8 km/sec and a thickness of 1.0 km overlying a 1-km-thick layer with a velocity of 4.6 km/sec and a 1-km-thick layer with a velocity of 5.0 km/sec. Below 3 km, the velocity model is similar to the regional Cascade Range velocity model discussed by W. M. Kohler, J. H. Healy, and S. S. Wegener [*J. Geophys. Res.* **87**, 339 (1982)].
8. All the earthquakes examined in this study have at least seven well-recorded P-wave arrivals, root-mean-square travel time residuals of less than 0.25 second, and calculated errors of less than 1.5 km in all three dimensions. The actual resolution of the hypocenters for the shallow volcanic earthquakes (depths < 2.5 km) is about 1 km.
9. The calculation of seismic energy released at Mount St. Helens is discussed by Malone *et al.* (*4*). These investigators consider the problems of identifying changes in the shape of the energy release curve but do not explicity divide the accumulated $(E_s)^{1/2}$ curve into the two phases discussed here. Both the initial constant increase and the final step increase phase discussed here are clearly evident for most of the nine eruptions plotted in figure 2 of (*4*).
10. The scarp mapped immediately north of the lava dome [figures 2 and 3 of (*5*)] may be the surface expression of the fault hypothesized in our model on the basis of the earthquake locations and focal mechanisms.
11. A number of investigators have proposed that a shallow magma body was emplaced during the cataclysmic eruption on 18 May 1980 [P. W. Lipman, D. R. Norton, J. E. Taggart, Jr., E. L. Brandt, E. E. Engleman, *U.S. Geol. Surv. Prof. Pap. 1250* (1981), p. 631].
12. K. V. Cashman and J. E. Taggart, *Science* **221**, 1385 (1983).
13. T. Casadevall *et al.*, *ibid.*, p. 1383.

14. We appreciate the many hours that S. Carlson and J. Terreberry worked in support of the prediction effort during the eruption sequence of February to March 1982 and the assistance of W. Grant in the reexamination of the earthquake data.

26 January 1983; revised 27 June 1983

Eruption-Triggered Avalanche, Flood, and Lahar at Mount St. Helens—Effects of Winter Snowpack

Abstract. *An explosive eruption of Mount St. Helens on 19 March 1982 had substantial impact beyond the vent because hot eruption products interacted with a thick snowpack. A blast of hot pumice, dome rocks, and gas dislodged crater-wall snow that avalanched through the crater and down the north flank. Snow in the crater swiftly melted to form a transient lake, from which a destructive flood and lahar swept down the north flank and the North Fork Toutle River.*

Since the explosive eruptions of Mount St. Helens in 1980 (*1*), dacitic lava has erupted periodically to build a dome that in early 1982 rose some 200 m above the crater floor (Fig. 1). On 19 March 1982, a dome-building eruption began with an explosive phase. Had the eruption occurred in summer, the destructive effects of the relatively small explosive eruption would have been confined to the crater and the upper flanks of the volcano. But because snow thickly mantled the steep crater wall, a lateral blast generated a large avalanche that flowed 8 km off the volcano. Heat from eruption products meanwhile swiftly melted snow, producing a transient lake whose sudden discharge extended effects of the eruption far downvalley. The complex sequence of eruptive and flow events—probably all occurred within a few minutes—are inferred from stratigraphic field relations gathered within a few days of the eruption and from geophysical data and distant visual observations.

Glowing projectiles were observed above the crater rim from an aircraft 35 km south of the volcano at about 1927 P.S.T. (0027 U.T., 20 March), roughly the time of the seismic onset of the eruption (*2*). The projectiles apparently were part of a blast of hot juvenile pumice, dome rocks, and gas that erupted from the south side of the dome. Two or 3 minutes later, a central eruption column rose to an altitude of 13.6 km (*3*); wind carried the plume southeast, depositing pumice on the southeast flank of the volcano and beyond. The absence of pumice on the dome indicates that both the lateral blast and the vertical column were directed away from the dome, probably from a vent low on its south flank or adjacent crater floor (*4*).

The lateral blast dislodged most of the snow from the precipitous, 500-m-high crater wall in the 120° sector east through south-southwest. The snow and injected rocks avalanched down the steep wall. Snow that remained high on the crater wall after the eruption was studded with angular blocks; snow remaining near the base of the wall had become deeply fluted and grooved by the avalanche.

The avalanche split and flowed around both sides of the dome, joined 400 m farther north in the axis of the breach, descended the north flank of the volcano, and swept across the pumice plain to Spirit Lake and the North Fork Toutle River (Figs. 1 and 2). The volume of the avalanche was 10^6 to 10^7 m^3. Its velocity, calculated from run-up and superelevation of deposits (*5*), varied with slope and with distance from the crater. The avalanche accelerated down the crater wall to about 70 m/sec. Running down the gentle crater floor and breach, the avalanche gradually slowed to 10 m/sec but then accelerated to about 16 m/sec as it descended the steps and north flank of the cone. On the pumice plain it slowed to 6 m/sec and less. The maximum distance traveled was 8.4 km; the approximate center of mass was displaced 5.5 km. The fahrböschung (*6*) was about 9°, suggesting an average apparent coefficient of friction of about 0.16.

Along its axis the avalanche eroded through the snowpack in the breach and into pumice and rockfall deposited in 1980 and 1981. But near its lateral margins the avalanche was much less erosive; locally it plowed up large snow blocks, but in general it barely disturbed the snow, over which it laid deposits 0.1 to 1 m thick. In a few places near its margins, the avalanche descended into fumarole-melted caves in the snowpack. After descending the steps, the avalanche decelerated and spread out on the pumice plain, depositing snow and lithic debris as thick as 3 m over several square kilometers. The margins of the deposits were steep-fronted lobes 0.3 to 1 m high, where pumice blocks were concentrated.

The avalanche deposit typically was a nonsorted, nonstratified mixture, half corn-snow granules and half pumice and rock fragments. Downslope it was progressively enriched in rock fragments, owing to the incorporation of scoured material. The poorly sorted fragments of pumice and rock, ranging from clay to boulder size, made the deposit dark gray (Figs. 1 and 2). The initial porosity of the deposit was about 40 percent; the 1-mm median grain size of snow granules in the avalanche deposit was similar to that of undisturbed snow in the crater. Weeks later when the snow had melted, the deposit had settled to a nonsorted, nonstratified, light-gray, dry, pumiceous sandy gravel only 1 cm to 1 m thick.

Certain characteristics of the deposit before its snow component had melted suggest that the avalanche behaved variously as a dry flow and as a brittle slide. The thinness of the distal deposit, its lobate form, the concentration of large low-density blocks at the margins, and the long runout distance suggest a dominantly dry-flow style of movement (*7*).

But locally abundant longitudinal and transverse shear surfaces imply brittle deformation in places rather than flow.

Except in the crater, the only evidence that the avalanched snow melted during or just after emplacement (ambient air temperature was below 0°C) was a freezing together of the corn-snow granules of the deposit. Apparently heat of internal friction and the warmth of the pumice blocks caused incipient melting during the avalanche. Only the largest pumice blocks were still warm 15 hours after the avalanche.

A transient, crescent-shaped lake developed between the dome and crater wall as a result of the melting of snow on the crater wall and floor, and probably of snow that the avalanche had piled behind the dome. Melting was caused by hot pumice fragments in the avalanche deposit, by hot gas, radiant heat, and possibly hot water from the vent, and probably by continuous ejection of hot pumice. Evidence for the lake just after the eruption included strandline accumulations of floated pumice blocks and lapilli, stranded blocks of granular snow, and horizontal upper limits of mud-saturation of freshly caved snow (Fig. 3). Strandline deposits consist of subangular to subround openwork pumice blocks that form horizontal benches as high as 15 m above the irregular crater floor, a level indicating that the maximum volume of the lake was about 4×10^6 m^3. Several other strandline benches formed 2 to 8 m below the maximum strand. Small deltas just below the highest strand were deposited by streams of water flowing into the lake from melted snow on the crater wall (Fig. 3). A horizontal upper limit of mud formed on freshly truncated snow just below the level of the highest pumice strand. Only below this sharp limit was the snow conspicuously fluted by melting and permeated with brown mud. Scattered blocks of granular snow as large as 4 m, also fluted by melting and permeated with mud, were stranded on the crater floor below the maximum lake level.

The area of the transient lake in the moat between the dome and the crater walls became floored by juvenile pumice blocks, lapilli, ash, and sparse lithic fragments. On parts of the crater floor these thick deposits collapsed to form depressions as broad as 100 m and deep as 10 m, some of them outlined by concentric, infacing scarps. The collapse scarps, probably caused by melting of the thick preeruption snowpack beneath the warm pumice deposit, expose partial sections of deposits that grade upward from dense lithic and pumice blocks in an ash matrix, to pumice and ash, to ash; this 3- to 5-m sequence is capped by 1 to 3 m of very low-density openwork rounded pumice blocks. The lower part of the deposit apparently formed by materials settling through water, the upper part by the accumulation of floating pumice blocks stranded as the lake drained. The floating pumice blocks had abraded each other, becoming rounded and producing the ash that settled to the lake bottom.

The lake had outlets both east and west of the dome; no remnants of any dam material occur at either outlet. Each condition, especially the unusual circum-

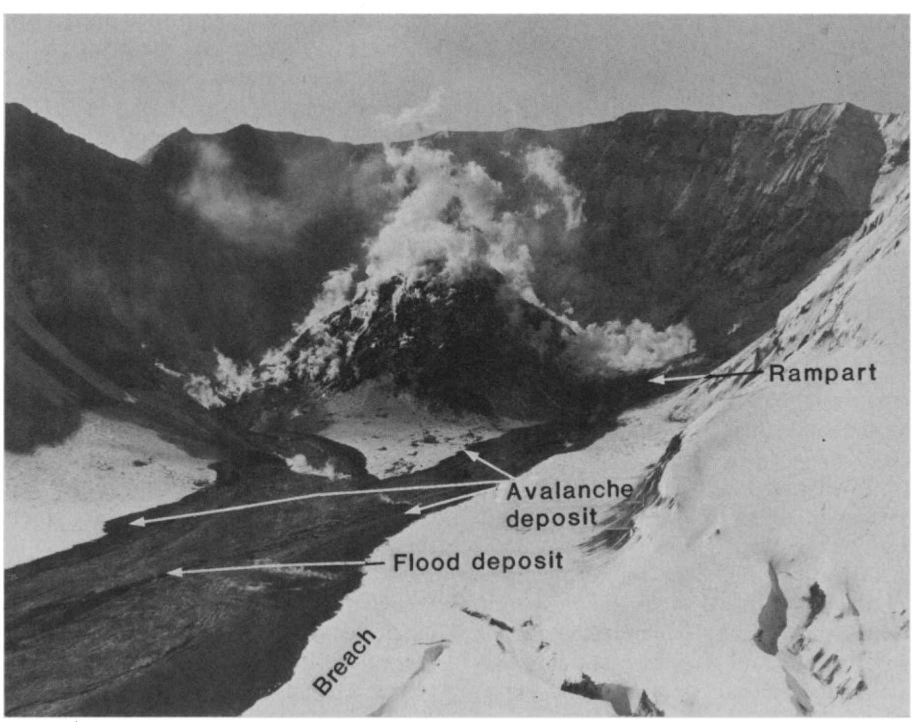

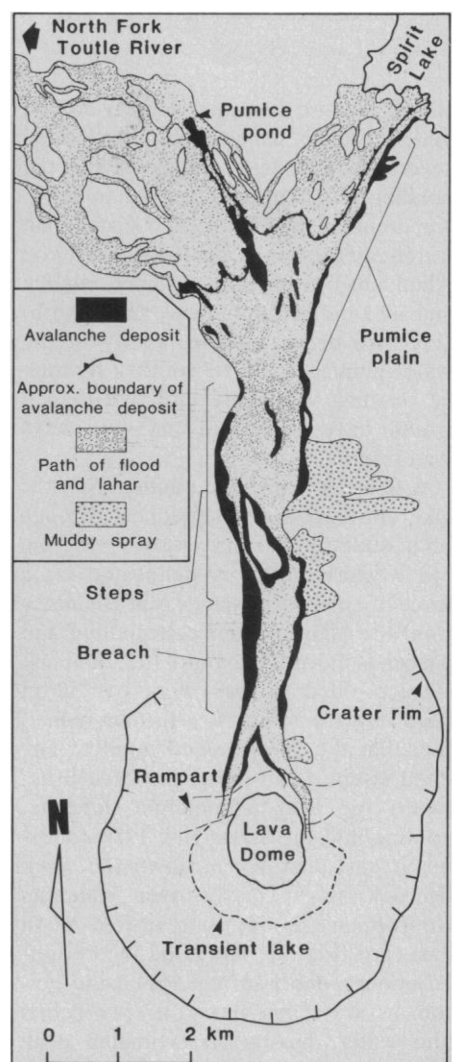

Fig. 1 (left). View southward of the crater on 23 March 1982. Arms of flood and avalanche deposits descend across the rampart north of the dome and merge on the floor of the breach. The lithic and pumiceous snow-avalanche deposit is the dark-colored material that encloses the broad, flood-scoured gully in the center. Fig. 2 (right). Map of the effects produced by lithic and pumiceous snow-avalanche and the succeeding flood and lahar on 19 March 1982.

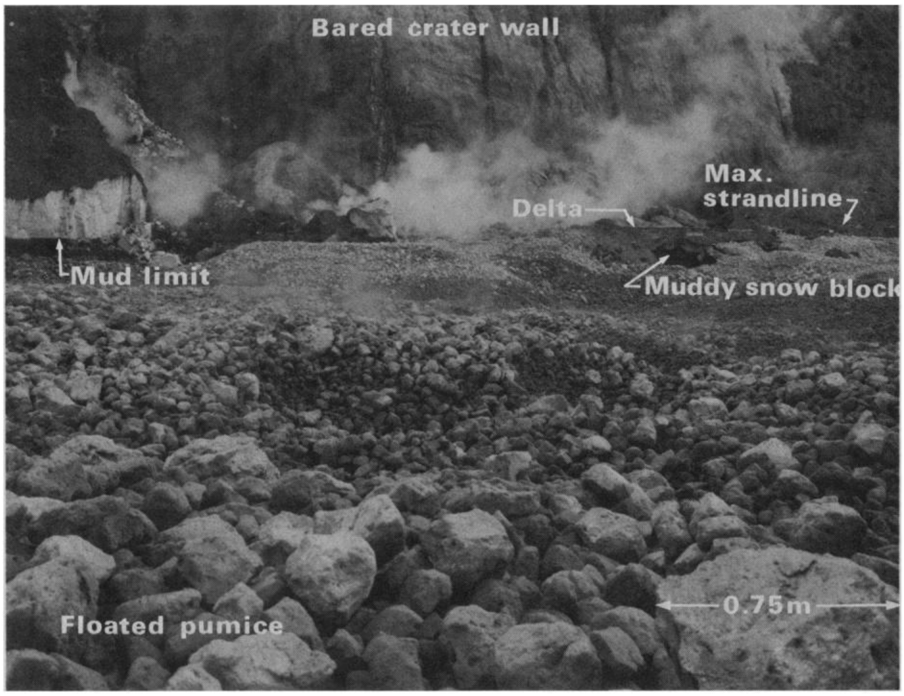

Fig. 3. View southwest across the pumice-filled crater floor on the south side of the dome. The nearby small delta and the horizontal upper limit of mud on freshly caved snow roughly coincide with the pumice strandline. Subangular to subround pumice blocks in the foreground and the large dark-colored snow blocks were stranded during the draining of the lake. The bared crater walls had been covered with snow just before the eruption.

stance of more than one scarcely eroded outlet through which water discharged several meters deep, indicates that the ponding was hydraulic and dynamic (*8*). Apparently the snow melted faster than water could escape from the two outlets. Abundant floating and entrained pumice and ash, and perhaps slushy snow, probably also decreased the fluidity of the water-pumice mixture so that hydraulic ponding was more effective than it would have been had the fluid been water only.

A flood of water and pumice from the lake discharged simultaneously through both outlets. The maximum flow from the western outlet is delineated by a levee of openwork pumice that emanates from the highest pumice strandline and descends northward onto the rampart. Vertical-sided ravines were cut 30 m deep into the rampart, a further indication that the lake drained rapidly. The flood swept down the crater breach between the avalanche-margin deposits, eroding into the underlying 1980 deposits. It cascaded 400 m down the steep bedrock steps, partly over cataracts from which a muddy spray drifted 700 m eastward (Fig. 2). The flood incorporated enough debris to emerge at the bottom as a viscous slurry of rock debris and water, having an estimated peak discharge of at least 13,800 m^3/sec (about 4 m deep, 230 m wide, with a velocity of 15 to 20 m/sec) (*9*). Transformation of the flood into a lahar is inferred from the poorly sorted, nonstratified, matrix-rich deposit below the steps. The lahar flowed as a broad sheet across the pumice plain, where it divided. One arm entered Spirit Lake, but most of it flowed in anastomosing channels across the hummocky surface of the 1980 debris-avalanche and pyroclastic-flow deposits and then into the North Fork Toutle River (Fig. 2).

Erosion and deposition by this flow destroyed much of the surface morphology of the 1980 pyroclastic-flow deposits. The flow filled the former "pumice pond" and overflowed its west rim, where the flow cut a ravine deep enough into still-hot 1980 pyroclastic-flow deposits to generate small phreatic explosions, which deposited fine ash around the ravine. Rapid headward recession of cataracts caused the pumice pond and other parts of the plain to integrate with the North Fork Toutle drainage for the first time since earlier drainage lines were obliterated by the great debris avalanche and pyroclastic flows of 18 May 1980 (*1*). Channels resurveyed as far as 35 km from the crater had incised by 5 to 11 m.

Two lithologically distinct surges of the lahar flowed as slurries for at least 35 km down the North Fork Toutle Valley. The first was gray with a sandy matrix consisting primarily of lithic clasts; the second was brown and pumice-rich with a muddier matrix. Velocities computed from superelevations at bends along this reach were 4 to 9 m/sec (*5*); sediment concentrations, experimentally determined from reconstituted samples (*10*), ranged from 75 to 90 percent (by weight). The deposits, which remained liquefied for more than a day, were poorly sorted and nonstratified, typical of laharic deposits (*11*).

Beyond 35 km from the crater, laharic deposits are better sorted, stratified, and depleted in silt and clay as compared to deposits upvalley. During the flow, sediment concentrations at stream-gauging stations 58, 73, and 81 km downstream from the crater were progressively more dilute [71, 67, and 61 percent (by weight) solids, respectively], and peak discharge decreased progressively (960, 650, and 450 m^3/sec) even though flow velocities remained 4 to 6 m/sec. These data, eyewitness accounts of standing waves at these stations, and the inability of fresh deposits there to retain their interstitial water (*12*), suggest that the lahar gradually became a hyperconcentrated water flow. Beyond 35 km from the crater, channels aggraded, in contrast to the notable downcutting that occurred upvalley. By the time the flow reached the Cowlitz River confluence 84 km from the crater, it was so dilute that it produced only a 25-cm rise in the river at a nearby gauging station.

Peak discharge was an order of magnitude less than that of lahars that had devastated the Toutle River Valley on 18 May 1980. Nonetheless, the 1982 lahar breached and severely eroded a debris-retention dam 35 km from the crater and caused extensive deposition throughout the lower Toutle River. Mudlines of 19 to 20 March 1982 were only a few meters below those of the great 18 May 1980 lahar, because aggradation during winter storms in 1981 and 1982 had severely reduced channel capacity. As long as Mount St. Helens remains active, a potential exists for large snow avalanches, floods, and lahars to be destructive far from the vent.

R. B. WAITT, JR.
T. C. PIERSON
N. S. MACLEOD
R. J. JANDA
BARRY VOIGHT
R. T. HOLCOMB

U.S. Geological Survey, Cascades Volcano Observatory, Vancouver, Washington 98661

References and Notes

1. *U.S. Geol. Surv. Prof. Pap. 1250* (1981).
2. C. S. Weaver and S. D. Malone, personal communication.
3. According to U. S. Weather Service radar at Portland, the eruption column reached its maximum height, 11.5 km above the vent, at 1930 P.S.T. Maximum radar reflection lasted only 5 minutes; the plume then gradually descended and drifted south-southeast. Pumice in flow deposits in and north of the crater appears identical to that which fell from the plume onto the south flank of the volcano.
4. D. A. Swanson, personal communication. A small part of the dome low on the south sector disappeared during the eruption as a result of explosion or collapse; this location may mark the approximate position of the principal vent.
5. Velocity is calculated from superelevation flood surfaces at channel bends by the formula $v^2 = rg \tan \Theta$, where v is the velocity of ideal fluid, r is the radius of curvature at the bend, g is the acceleration due to gravity, and Θ is the angle between the superelevated flow surface and the horizontal, measured normal to the flow direction.
6. Fahrböschung is given by arctan (H/L), where H is the maximum vertical fall and L is the maximum horizontal runout [A. Heim, *Bergsturz und Menschenleben*, Fretz und Wasmuth, Zurich, 1932)]. The parameter has been used by Heim and by others as an index of the average apparent coefficient of friction: $f = H/L$ [W. G. Pariseau and B. Voight, in *Rockslide and Avalanches*, B. Voight, Ed. (Elsevier, Amsterdam, 1979), vol. 2, pp. 6–8]. By comparison, debris avalanches at Sherman Glacier, Gros Ventre, and Mount St. Helens (18 May 1980) have fahrböschung-derived coefficients of friction of 0.22, 0.17, and 0.09 to 0.15, respectively.
7. K. J. Hsü, *Geol. Soc. Am. Bull.* **86**, 129 (1975).
8. Hydraulic ponding occurs in an unblocked open channel if water is supplied more rapidly than it can be discharged; water level therefore rises until outflow equals inflow, perhaps only after the channel sides are overtopped and multiple outflows are thus created. The outstanding geologic example of hydraulic ponding in Washington is due to enormous Pleistocene floods from glacial Lake Missoula, which became transiently hydraulically ponded by each successive constriction in the Channeled Scabland and Columbia River Valley [J H. Bretz *et al.*, *Geol. Soc. Am. Bull.* **67**, 957 (1956); V. R. Baker, *Geol. Soc. Am. Spec. Pap. 144* (1973); R. B. Waitt, Jr., *J. Geol.* **88**, 653 (1980)].
9. The velocity of the lahar was estimated by comparison with 18 May 1980 lahars of similar magnitude, composition, and slope angle, for which velocities were computed [R. J. Janda *et al.*, in (*1*), p. 464].
10. One can estimate the original water content of a lahar by adding enough water to dry samples to produce a slurry that has the consistency of fluid, wet concrete. The method, although subjective, is relatively precise. A decrease in water content of only 1 to 2 percent from optimum renders the slurry too viscous to flow; an increase of 1 to 2 percent so dilutes the slurry that it cannot hold coarse particles in suspension.
11. See D. R. Crandell, *U.S. Geol. Surv. Prof. Pap. 677* (1969).
12. R. L. Dinenart, personal communication.

26 January 1983; revised 30 June 1983

Peru Coastal Currents During El Niño: 1976 and 1982

Abstract. *Year-long measurements of subsurface current and temperature on Peru's continental shelf included the onset of El Niño in 1976 and 1982. The Peru Coastal Undercurrent more than doubled in speed and advected anomalously warm water poleward. El Niño began in different seasons in 1976 and 1982, but the current and temperature responses were very similar. Acceleration of poleward flow at 10°S occurred several days after sea level rose at the Galápagos Islands in October 1982, suggesting the onset of El Niño propagated as a Kelvin wave.*

El Niño is, among other things, the appearance of anomalously warm water along the coasts of Ecuador and Peru, with disastrous ecological and economic consequences. Its causes and effects have been traced at least as far as the western equatorial Pacific (*1–3*), but its manifestations are especially dramatic in the Peruvian littoral (*4*). Neither the 1976 nor 1982 El Niño was predicted, but long-term measurements of subsurface current and temperature recorded the onset of El Niño on Peru's continental shelf (Fig. 1) in both years. Although the measurements were obtained at different locations and depths on the shelf (55 m below the surface over the 120-m isobath at 15°S during March 1976 to May 1977; 100 m below the surface over the 150-m isobath at 10°S during November 1981 to January 1983), both were in the Peru Undercurrent, which flows poleward (southeastward) along the coast. This poleward flow occurs over the continental shelf and slope (*5*), just beneath the layer of water driven equatorward and offshore by the wind, supplying the water that upwells along the coast of central Peru (*6*). The time series of subsurface temperature, current, and coastal wind are shown in Figs. 2 and 3 (*7*). Except for warming occurring in different seasons, the time series are remarkably similar (*8*). The coastal winds were persistently favorable for coastal upwelling (*6*), and increased during the warming phases (*9*).

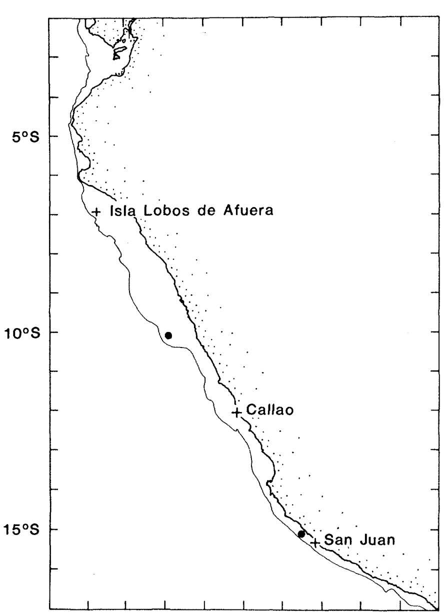

Fig. 1. Current meter locations off Peru (two bold dots) and the 200-m isobath, approximate edge of the continental shelf. Winds were measured at Isla Lobos de Afuera and San Juan and SST's were measured at Callao.

To place these measurements in temporal and climatological perspective, the monthly mean sea surface temperatures (SST's) at Callao (12°S) are shown in Fig. 4. In a normal year, seasonal warming begins around October and continues until March. However, El Niño occurs at irregular intervals of several years (*1, 2*). The associated anomalous warming along the Peruvian coast usually begins in February or March after anomalous weakening of the westward trade winds in the western and central equatorial Pacific starting the previous October or November (*1, 2*). This sequence occurred in late 1975 and early 1976, but in 1982 the equatorial trade winds severely weakened in the early part of the year (*2*) and anomalously strong warming began along the coast in October 1982.

The onset of El Niño conditions in 1976 and 1982, apparent in the monthly SST data and in the subsurface temperature time series, coincided with increased poleward flow. In 1976 the temperature at 55 m rose by 3.5°C (from 13.6° to 17.1°C) during the first 64 days of the time series (27 March to 30 May); the mean alongshore current was 23.2 cm sec^{-1} poleward during that period. In contrast, during a comparable period after the return to nearly normal conditions (the last 64 days of the time series almost 1 year later: 10 March to 13 May 1977), the temperature remained near 15°C and the mean alongshore current was only 8.8 cm sec^{-1} poleward. In 1982 the temperature 100 m below the surface at 10°S rose 5.7°C (from 15.0° to 20.7°C) during the 64 days from 7 October to 10 December; during that period the mean alongshore current was 25.3 cm sec^{-1} poleward. During an equivalent period nearly 1 year earlier (23 November 1981 to 26 January 1982), the temperature increased less than 1°C from 13.8°C and the alongshore current was only 4.4 cm sec^{-1} poleward.

The anomalous warming in 1976 and 1982 was gradual and continuous for at least 4 months, and the current was strongly poleward from the beginning of the warming. This suggests that the subsurface warming was the result of advection by the poleward current. The temperature increase ($\partial T/\partial t$) of roughly